

LUNAR BASALTIC VOLCANIC ERUPTIONS: GAS RELEASE PATTERNS AND VARIATIONS IN LAVA VESICULARITY: 2. FISSURES, MARE FLOWS, AND RING MOAT DOME STRUCTURE (RMDS) MORPHOLOGY. L. Wilson¹ and J. W. Head² ¹Lancaster Environment Centre, Lancaster University, Lancaster LA1 4YQ, U.K. (l.wilson@lancaster.ac.uk), ²Department of Earth, Environmental and Planetary Sciences, Brown University, Providence, RI 02912, U.S.A. (james_head@brown.edu).

Introduction: In a companion abstract [1] we outline 4 phases expected to have occurred during a typical lunar volcanic eruption. These are Phase 1: arrival of a dike from the deep mantle which releases gas and magmatic foam in a transient but vigorous explosive eruption forming regional pyroclastic deposits; Phase 2: a high volume flux, hawaiian-style eruption forming an at least partly optically dense fire-fountain from which pyroclasts efficiently lose volatiles and accumulate to form non-vesicular lava. This phase continues until the dike reaches a buoyancy equilibrium between the crust and mantle densities and ceases to ascend. Phase 3 begins as the dike is squeezed by relaxation of the internal excess pressure holding the dike open, forcing magma to the surface at a decreasing volume flux. With a stable internal pressure gradient in the dike, magma volatile exsolution deep in the dike becomes negligible and gas bubbles rise and coalesce to produce strombolian activity until all of the deep-sourced CO gas has been lost. Phase 4 now involves release of H₂O and S compounds in shallow magma as it is forced upward. Surface tension stabilizes small (~20 μm) gas bubbles against exploding into the overlying vacuum and a stable crust forms on lava leaving the vent. This phase continues at an exponentially decreasing volume flux until dike stresses are completely relaxed. This outline of the sequence of events expected in basaltic lunar eruptions is generic: all phases should have occurred in all eruptions. However, the relative importance and duration of the various phases varied significantly, being dictated by the total magma volatile inventory, the global state of stress in the lithosphere, and the consequent way in which the erupted magma volume flux changed with time.

In [1] we identified four different configurations that commonly result from eruptions: 1 - Summit pit craters on shield volcanoes (e.g., Ina); 2 - Calderas associated with intersecting dikes (e.g., Hyginus); 3 - Linear depressions above dikes (e.g., Sosigenes); and 4 - Topographically uncontained linear vents above fissure eruptions in the maria (e.g., most mare IMPs). Also in [1] we addressed the first two of these configurations, in which all three of the magma volatile content driving explosive activity, the active length of the fissure vent, and the erupted magma volume flux were relatively small. Low volatile content and short fissure length caused pyroclasts to be ejected approximately radially to only a few km, producing optically dense fire fountains

from which uncooled pyroclasts accumulated to form lava ponds at magmatic temperatures. The ponds overflowed to feed lava flows, and the low magma volume fluxes ensured that these were short, cooling-limited flows that accumulated to form small shield volcanoes with summit pits. Fractures in the crusts of the lava ponds allowed underlying extremely vesicular foam to erupt to form low domes [2, 3], these being one sub-set of the features called irregular mare patches (IMPs) [4]. We now consider configurations 3 and 4, involving the longer fissure vent outcrops and higher magma volume fluxes needed to explain the properties of large-scale mare lava flows.

Mare volcanism: The low viscosities of lunar basalts coupled with typical thicknesses of 20-50 m [5] for large >100 km long mare lava flows emplaced on surface slopes of order 10⁻³ imply typical flow speeds of 10-20 m s⁻¹ and inevitably require turbulent rather than laminar motion in the proximal parts of flows [6, 7]. Turbulence inhibits formation of a stable surface crust and maximizes radiative heat loss. Even so, analyses of turbulent lavas eroding lunar sinuous rille channels show that turbulence will persist in such thick flows until the lava has traveled for at least ~100 km [8]. This implies that the lengths of most large mare flows were limited by the volume of magma available to be erupted rather than by cooling [5]. Vents feeding the larger mare flows are commonly hard to identify, but the ~30 km widths of the flows suggest that their fissure vents had outcrop lengths of ~10 km. Volume fluxes consistent with thicknesses, widths and flow speeds of lavas range from 10⁴ to 10⁶ m³ s⁻¹. We now assess how the successive eruptive phases outlined above influenced the lava emplacement process.

Phase 1. The very transient release of gas and foam concentration would have had minimal consequences, mainly depositing a thin layer of sub-mm pyroclasts over a large area around the vent.

Phase 2. This would have involved the formation of a relatively steady, largely optically dense hawaiian fire fountain within which sub-mm sized pyroclastic droplets would have lost gas efficiently and accumulated with negligible cooling in a linear zone a few to 10 km wide on either side of the fissure to form vesicle-free lava. This lava would have flowed away in an initially turbulent manner to form the distal part of the eventual lava flow deposit. This phase would have continued until the rising dike had established a neutral buoyancy

configuration relative to the crust-mantle boundary. The relative vertical extents of typical mantle dikes (50-90 km [5]) and the crust (~30 km [9]) imply that 40% to 70% of the total dike magma volume would have been erupted during this phase.

Phase 3. A decrease would now have occurred in magma rise speed and volume eruption rate as the dike ceased rising *en masse* towards the surface and instead began to shrink in thickness as the internal excess pressure holding the dike open was lost. There is no evidence in the morphologies of flows for a dramatic and abrupt decrease in eruption rate as this transition took place and to maintain the 10^4 to 10^6 $\text{m}^3 \text{s}^{-1}$ effusion rates the time constant for the presumably roughly exponential decrease in discharge is of order a few weeks. The low magma rise speed towards the end of this period would have allowed bubbles of exsolved CO gas formed at great depths [10] to move at an appreciable speed relative to the magmatic liquid being squeezed out of the dike and so coalescence of bubbles should have occurred, causing a change from hawaiian to strombolian explosive activity at the surface. The stabilization of the dike magma pressure distribution meant that no additional CO was released at depth and minimal amounts were released near the surface [10].

Phase 4. With minimal explosive release of CO gas now taking place, and a significantly reduced volume flux allowing laminar flow, a stable crust would have formed on the lava near the vent. The magma being erupted would have consisted of liquid containing bubbles of H₂O and sulphur species released over the last <500 m of magma rise [10]. These bubbles would have nucleated with diameters of ~10-20 μm and would have grown to ~20-30 μm at the surface, remaining stable as surface tension forces [2] imposed a pressure of ~70 kPa. Lunar basalts exsolving ~1000 ppm of H₂O and sulphur species would have left the fissure vent as lava foams with vesicularities up to 96% by volume.

Implications for vent areas: It is difficult to predict what fraction of the original volume of magma in a dike would have been erupted as foam, because both the extent and speed of the dike closure process would have been functions of the lithosphere stress regime, likely compressive late in the history of mare volcanism [11], and upper mantle rheology. Nevertheless the lava closest to the vent is likely to have been the most vesicular. The very last stages of activity at a vent would involve a competition between (i) cooling of un-erupted magma in the dike causing a reduction in volume and allowing drain-back of the last-erupted lava into the fissure and (ii) the final total relaxation of stresses forcing foam magma upward, possibly fracturing the crust on lava in the vent and extruding small foam flows as at Sosigenes

[12] (Fig. 1). Alternatively, these processes may have essentially cancelled one another out, leaving no clear topographic marker of the vent location, other than modification of the most vesicular lava near the vent by thermal and impact processes to form clusters of IMPs.

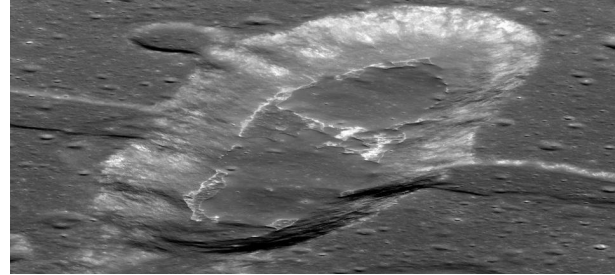


Figure 1. Oblique view of Sosigenes IMP. Modified from NASA LROC image NAC M1108117962LR.

Post-eruption changes in flows: After the main phases of an eruption are complete and all motion has ceased, changes still occur. Cooling of lava takes place at all boundaries, causing contraction stresses in the surface crust. Shrinkage of the lava as its density increases, being greatest where lava has infilled pre-eruption depressions, adds differential stresses. Crystallization due to cooling increases the concentration of residual volatiles in the magmatic liquid causing supersaturation and additional gas bubble nucleation. Where this process occurs in regions of a flow that already contain a foam core, expansion of the foam and extrusion of foam through cracks onto the lava flow surface can occur. This is a likely explanation of the ring moat dome structures [RMDSs, 13, 14] found in large numbers on many mare flows (Fig. 2). The moat surrounding the low dome structure represents loading and conservation of volume as the extrusion occurs.

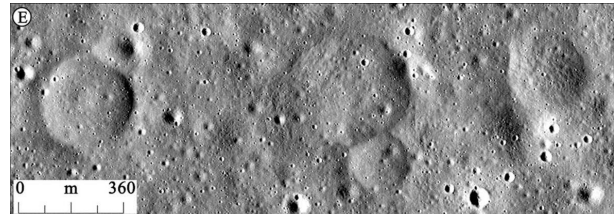


Figure 2. Ring moat dome structures in Mare Tranquillitatis, typically 4-6 m high. From Fig. 1E of [13].

References: [1] Wilson L. & Head J.W. This meeting. [2] Wilson, L. & Head, J.W. (2017) *JVGR*, 335, 113-127. [3] Qiao, L. et al. (2017) *Geology*, 45, 455-458. [4] Braden S.E. et al. (2014) *Nature Geosci.*, 7, 787-791. [5] Hiesinger H. et al. (2002) *GRL*, 29, 1248, 4 pp. [6] Wilson L. & Head J.W. (2017) *Icarus*, 283, 146-175. [7] Head J.W. & Wilson L. (2017) *Icarus*, 283, 176-223. [8] Williams D. A. et al. (2000) *JGR*, 105, 20189-20205. [9] Wieczorek M. A. et al. (2013) *Science*, 339, 671-675. [10] Rutherford M. J. et al. (2017) *Amer. Mineral.*, 102, 20145-2053. [11] Solomon S. C. & Head J. W. (1980) *Rev. Geophys. Space Phys.*, 18, 107-141. [12] Qiao L. et al. (2017) *MAPS*, doi:10.1111/maps.13003. [13] Zhang et al. (2017) *GRL*, 44, 9216-9224. [14] Zhang et al. (2018) This meeting.